View metadata, citation and similar papers at core.ac.uk
brought to you by CORE
provided by Ghent University Academic Bibliography

# 0.3pA Dark Current and 0.65A/W Responsivity 1020nm InGaAs/GaAs Nano-Ridge Waveguide Photodetector Monolithically Integrated on a 300-mm Si Wafer

Cenk Ibrahim Ozdemir[(1),(2),*], Yannick De Koninck[(1)], Didit Yudistira[(1)], Nadezda Kuznetsova[(1)], Marina Baryshnikova[(1)], Dries Van Thourhout[(1),(2)], Bernardette Kunert[(1)], Marianna Pantouvaki[(1)], Joris Van Campenhout[(1)]

[(1)] imec, Kapeldreef 75, 3001 Leuven, Belgium, [*]cenk.ozdemir@imec.be

[(2)] Photonics Research Group, INTEC, Ghent University, Technologiepark-Zwijnaarde 126, 9052 Ghent, Belgium

**Abstract** *We report p-i-n InGaAs/GaAs multi-quantum well nano-ridge waveguide photodetectors monolithically integrated on a 300-mm Si wafer. The devices exhibit low dark currents of 0.3 pA (1.36x10$^{-7}$A/cm$^{2}$) at -1V bias and internal responsivities of 0.65A/W at 1020nm wavelength.*

## Introduction

Silicon photonics (SiPho) attract interest for optical communications applications as it enables dense and high throughput integration of photonic devices at low cost. Active device capabilities such as amplification and detection are typically achieved in a SiPho platform by introducing additional materials, such as Ge or III-V materials. State of the art Ge-on-Si photodetectors (PDs) offer high responsivities and high bandwidth[1] but suffer from high dark currents reducing their sensitivities. Compared to III-V materials, Ge-on-Si is not versatile for other active capabilities such as light generation and amplification due to its indirect bandgap.

Lattice and thermal expansion mismatches challenge high quality monolithic III-V integration on Si. Yet, aspect-ratio trapping of misfit defects inside nano-trenches close to the III-V/Si interface can achieve low density of threading dislocations and planar defects, without depositing thick buffer layers[2]. Compared to other monolithic integration approaches, nano-ridge (NR) engineering enables evanescent optical coupling between the III-V waveguide and an underlying Si waveguide[3], due to the close proximity of the III-V waveguide to the Si substrate, as well as III-V waveguide cross-sections with precisely controlled layer composition and thicknesses on top of the nano-trenches[4]. This approach has therefore the potential to realize a fully integrated SiPho platform with monolithic III-V light sources, electrooptic III-V modulators and III-V photodetectors (PDs). Recently, high quality III-V nano-ridge (NR) waveguides selectively grown on Si substrates have been shown to support optically pumped lasing[5]. In [6], we reported InGaAs/GaAs multi-quantum well (MQW) nano-ridge waveguide photodetectors (NRWPD) monolithically grown on a 300-mm Si substrate using the NR engineering method for the first time, exhibiting 10pA dark current, and 0.25A/W internal responsivity at -1V.

In this study, we demonstrate InGaAs/GaAs MQW NRWPDs with a dark current of ~0.3 pA at -1 V bias voltage at 1020 nm wavelength. This is almost 2 orders of magnitude lower than previously reported[6], and to the best of our knowledge the lowest dark current ever reported for a monolithic III-V on Si photodetector[7-9]. They exhibit internal responsivities (internal quantum efficiency) of 0.65 A/W (79%) at -1 V bias voltage at 1020 nm wavelength.

## Device Design and Fabrication

InGaAs/GaAs NRs are grown on patterned Si wafers in imec's 300-mm CMOS line. The InGaAs/GaAs NRs are epitaxially grown on n-doped Si using metalorganic vapor-phase epitaxy (MOVPE) and applying NR engineering in high-aspect ratio trenches with 100 nm width, which are etched into a silicon oxide layer. Misfit defects

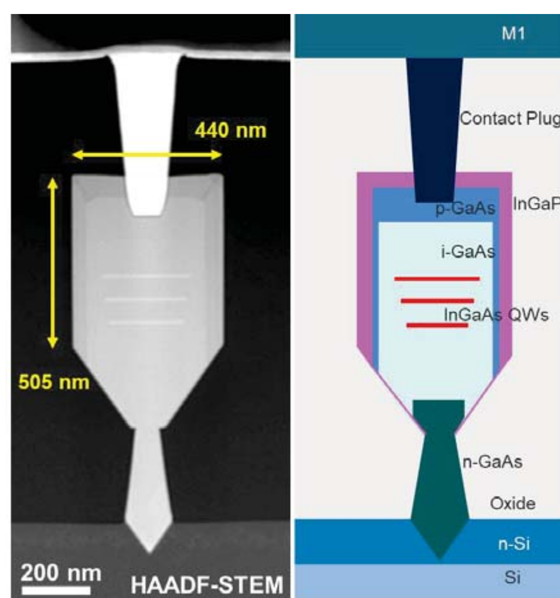


**Fig. 1** *(left)* HAADF-STEM cross-section image of GaAs nanoridge with 3x InGaAs QWs. *(right)* Schematic description of nanoridge cross-section.

initiated at the GaAs/Si interface are effectively confined inside the trenches[2]. A p-i-n diode is formed in the GaAs by introducing dopants during the epitaxial growth steps of GaAs. The nominal target doping concentrations are $5\times10^{18}$ $cm^{-3}$ and $1\times10^{19}$ $cm^{-3}$ for n-type and p-type GaAs, respectively. The active medium consists of three $In_{0.20}Ga_{0.80}As$ QWs of 10nm target thickness, embedded in the i-GaAs layer. The InGaAs/GaAs NR is then capped with an InGaP layer for surface passivation. After the oxide filling, the InGaP layer is locally etched and tungsten contact plugs were formed to electrically contact the top p-GaAs layer. Based on the design, p-contact plugs have different pitch distances on different devices. The n-GaAs was contacted via tungsten contact plugs connected to the n-doped Si substrate. The fabrication is completed using standard CMOS Cu metallization processing. A schematic cross section and transmission-electron microscopy (TEM) image of the final structure are shown in Fig. 1.

## Electrooptic Performance

The InGaAs/GaAs NRs are cleaved on one side to produce 500 μm long edge-coupled NRWPDs. Each cleaved edge gives access to 16 measured devices of 100 nm trench width. The pitch of the p-contacts to the p-GaAs was varied from 0.6 μm, to 1.2 μm, 2.4 μm, and 4.8 μm.

The electrical dark current-voltage (I-V) characterization of the InGaAs/GaAs NRWPDs reveals p-i-n diode behavior with more than 6-order of rectification (Fig. 2). Forward bias dark currents are dependent on p-contact plug pitches. The devices exhibit a very low dark current of 0.3 pA maximum at -1 V bias voltage, and 0.6 pA at -2V (Fig. 2). Considering the 440 nm width (measured on TEM images) and 500 μm length of the NRs, this corresponds to a $1.36\times10^{-7}$ $A/cm^2$ equivalent dark current density at -1 V, which is lower than the lowest reported dark currents of III-V PDs grown on Si[6-9], and 5-order lower than typical Ge-on-Si PDs[1]. It is important to note that the devices reported here have higher bandgap in this comparison. Table.1 benchmarks the dark current densities and responsivities of different material schemes.

The InGaAs/GaAs NRWPDs are electrooptically characterized by edge-coupling a 1020 nm single wavelength laser using a HI-1060 metal tapered lensed fiber with 2.0 μm mode field diameter (MFD) beam (Fig.3.c). The output power at the tip of the lensed fiber is measured to be +7.00 dBm (5.01 mW) at 1020nm. The lensed fiber MFD is verified during the active alignment step of the measurements.

Light current I-V measurements are shown in

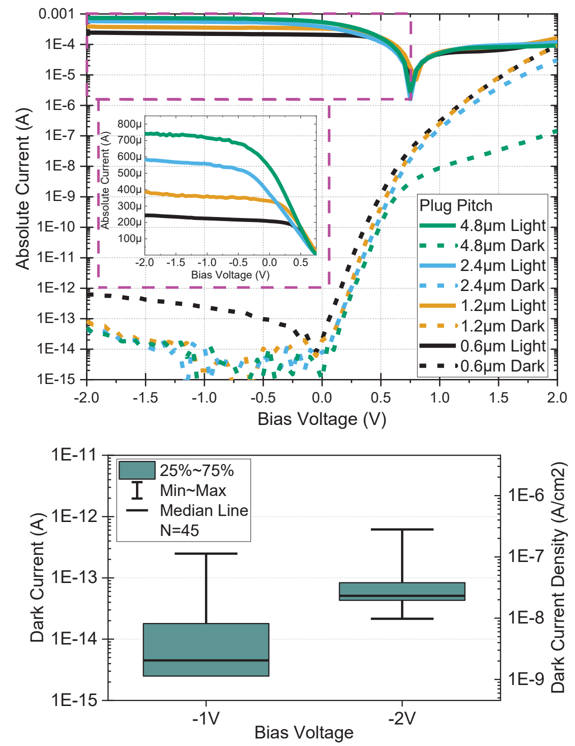


**Fig. 2**. *(top)* Dark and light IVs of devices with different p-contact plug pitches, (inset) light IV zoom in at linear scale. *(bottom)* Dark current distribution at different bias voltages.

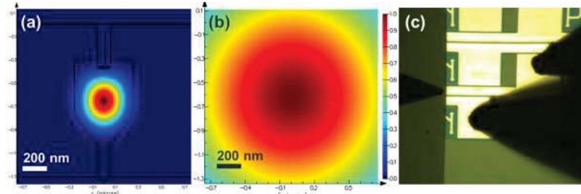


**Fig. 3** (a-b) Modal cross-sections of 100 nm trench width nanoridge and 2.0 μm MFD Gaussian beam, linear color scale. (c) Top view of measurement setup with cleaved facet and lensed fiber.

Fig. 2. More than 10-order of magnitude increase of the light compared to the dark current is observed at -1V for 4.8 μm p-contact plug pitch. Responsivity is reduced by the waveguide propagation losses. In the NRWPDs, given the dimensions of the PD cross section, the highly doped GaAs and the p-contacts are expected to contribute to these losses.

In order to evaluate the internal PD responsivity, the coupling efficiency $\eta_{coupling}$ of light from the lensed fiber into the NRWPD is simulated using Lumerical's finite difference time domain (FDTD) tool in 3D. The simulated MFD of the fundamental TE mode of the NR is 0.42 μm, while the MFD of the focused beam delivered by the lensed fiber is 2 μm, as shown in Fig. 3.a and -b. The coupling efficiency from the TE-polarized 2.0 μm MFD Gaussian beam of the lensed fiber into the NR is found to be 0.21. The coupled power, internal responsivity and internal quantum efficiency are then calculated with the formulas:

$$P_{coupled} = P_{out,lensed\ fiber} \times \eta_{coupling} \quad (1)$$

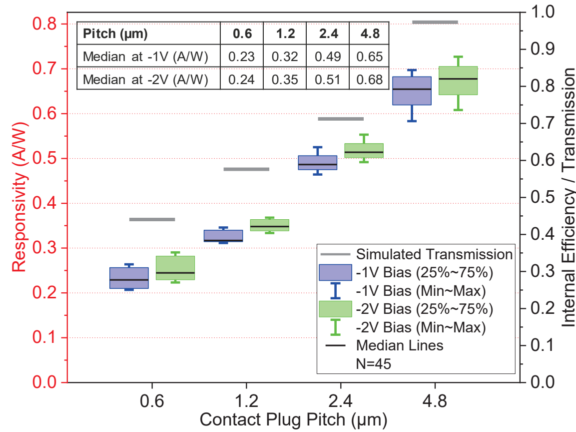


**Fig. 4** Responsivity distributions for different biases and p-contact plug pitches. Simulated transmission values for different p-contact plug pitches, scaled to right vertical axis. (Inset) Table of median responsivity values

$$R_{internal} = \left(I_{light} - I_{dark}\right)/P_{coupled} \quad (2)$$

$$\eta_{internal} = R_{internal}\hbar\omega/e \quad (3)$$

where $\hbar$ is reduced Planck constant, $\omega$ is frequency and $e$ is electron charge. The calculated internal responsivities for different p-contact plug pitch at -1V and at -2V bias are shown in Fig. 4. The highest responsivities are measured on the devices with 4.8 µm p-contact plug pitch. Due to small NR cross-section, mode field overlap with metal p-contacts increases with lower p-contact plug pitch, which largely increases the metal losses. Therefore, a clear dependence on the p-contact pitch versus responsivity is observed. The median internal responsivities (internal quantum efficiencies) of 4.8 µm plug pitch devices are measured to be 0.65 A/W (79%) at -1V and 0.68 A/W (82%) at -2V bias at 1020 nm laser wavelength (Fig. 5). In the light I-V measurements, light currents at reverse bias are observed higher than light currents at forward bias, which can be attributed to high input light power.

A second set of 3D FDTD simulations is completed to further investigate the effect of the p-contact plug pitch. This considers a uniform GaAs waveguide with no lossy material except the p-contact plugs. NRs with different p-contact plug pitches are excited with the fundamental TE-mode and the transmission is calculated after a

**Tab. 1:** Benchmark of Photodetectors Monolithically Integrated on Si

| Ref. | Mat. | V (V) | λ (nm) | R (A/W) | $J_{dark}$ (A/cm²) |
|---|---|---|---|---|---|
| [1] | Ge | -1 | 1310 | 0.93 | $3.4\times10^{-2}$ |
| [6] | III-V | -1 | 1020 | 0.45 | $1.4\times10^{-5}$ |
| [7] | III-V | -3 | 1550 | 0.79 | $8.0\times10^{-4}$ |
| [8] | III-V | -1.5 | 1346 | 0.4 | $1.4\times10^{0}$ |
| [9] | III-V | -5 | 1310 | 0.234 | $6.6\times10^{-5}$ |
| This work | III-V | -1 | 1020 | 0.65 | $\mathbf{1.4\times10^{-7}}$ |

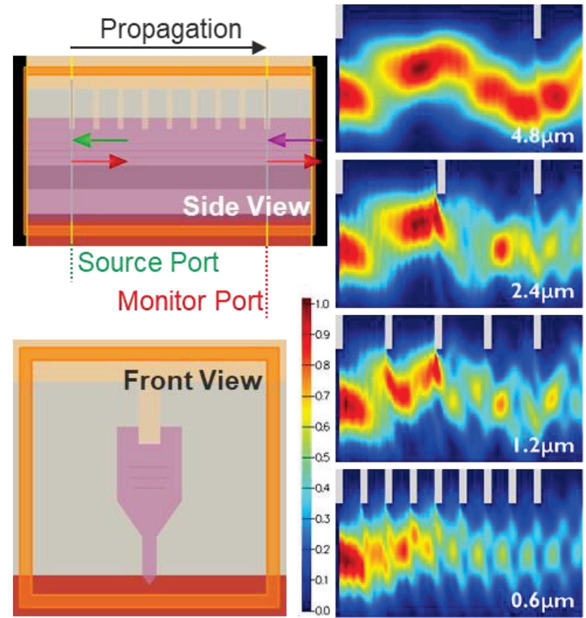


**Fig. 5** 3D FDTD simulations for calculating p-contact plug effects. *(left)* Side and front view of constructed simulation structure in Lumerical FDTD. *(right)* Side view of 2D power distribution at center for different p-contact plug pitches, grey plug shapes externally added for clarity

4.8 µm distance as shown in Fig. 5. The calculated transmission values are reported in Fig. 4 (grey lines). The internal responsivities follow this p-contact plug pitch dependence, suggesting that the drop in internal responsivities for smaller contact pitch values is linked to the loss induced by metal absorption. This result helps differentiating the responsivity reducing mechanisms of the NRWPD devices and can help further improve the device performance in future.

## Conclusion

p-i-n InGaAs/GaAs MQW photodetectors are monolithically grown on Si without thick buffer layers using the nano-ridge engineering approach. They exhibit record low median dark current of 0.3 pA ($1.36\times10^{-7}$A/cm² dark current density) at -1V, and 0.65 A/W median internal responsivity measured at 1020 nm wavelength for devices with 4.8 µm p-contact plug pitch . The p-contact plug density shows a trade-off between optical and electrical performance of the devices. This work shows the potential of III-V nano-ridge structures directly grown on Si as photodetectors for the monolithic III-V integration in a SiPho platform.


## Acknowledgment

This work was supported by imec's industry-affiliation Optical I/O R&D Program.


## References


[1] H. Chen *et al.*, "−1 V bias 67 GHz bandwidth Si-contacted germanium waveguide p-i-n photodetector for optical links at 56 Gbps and beyond," *Optics Express*,

vol. 24, no. 5, p. 4622, Mar. 2016, doi: 10.1364/OE.24.004622.

[2] M. Baryshnikova *et al.*, “Nano-Ridge Engineering of GaSb for the Integration of InAs/GaSb Heterostructures on 300 mm (001) Si,” *Crystals*, vol. 10, no. 4, p. 330, Apr. 2020, doi: 10.3390/cryst10040330

[3] Y. Shi, B. Kunert, Y. De Koninck, M. Pantouvaki, J. Van Campenhout, and D. Van Thourhout, “Novel adiabatic coupler for III-V nano-ridge laser grown on a Si photonics platform,” *Optics Express*, vol. 27, no. 26, p. 37781, Dec. 2019, doi: 10.1364/OE.27.037781.

[4] D. Van Thourhout *et al.*, “Nano-ridge laser monolithically grown on (001) Si,” in *Future directions in silicon photonics*, C. Jagadish, S. Lourdudoss, and J. E. Bowers, Eds. 2019, pp. 283–304.

[5] Y. Shi *et al.*, “Optical pumped InGaAs/GaAs nano-ridge laser epitaxially grown on a standard 300-mm Si wafer,” *Optica*, vol. 4, no. 12, p. 1468, Dec. 2017, doi: 10.1364/OPTICA.4.001468.

[6] C. I. Ozdemir *et al.*, “InGaAs/GaAs Multi-Quantum Well Nano-Ridge Waveguide Photodetector Epitaxially Grown on a 300-mm Si Wafer,” 2020 IEEE Photonics Conference (IPC), Sep. 2020, to be published.

[7] D. Inoue *et al.*, “Low-dark current 10 Gbit/s operation of InAs/InGaAs quantum dot p-i-n photodiode grown on on-axis (001) GaP/Si,” *Applied Physics Letters*, vol. 113, no. 9, p. 093506, Aug. 2018, doi: 10.1063/1.5041908.

[8] S. Mauthe *et al.*, “Ultra-Thin III-V Photodetectors Epitaxially Integrated on Si with Bandwidth Exceeding 25 GHz,” 2020, p. M3D.3, doi: 10.1364/OFC.2020.M3D.3.

[9] B. Chen *et al.*, “Low Dark Current High Gain InAs Quantum Dot Avalanche Photodiodes Monolithically Grown on Si,” *ACS Photonics*, vol. 7, no. 2, pp. 528–533, Feb. 2020, doi: 10.1021/acsphotonics.9b01709.